Electronic Supplementary Information for

High-index {hk0} faceted platinum concave nanocubes with enhanced peroxidase-like activity for ultrasensitive immunoassay

Zhuangqiang Gao, Shuzhen Lv, Mingdi Xu, and Dianping Tang*

Key Laboratory of Analysis and Detection for Food Safety (MOE & Fujian Province), Collaborative Innovation Center of Detection Technology for Haixi Food Safety and Products (Fujian Province), State Key Laboratory of Photocatalysis on Energy and Environment, Department of Chemistry, Fuzhou University, Fuzhou 350116, PR China

CORRESPONDING AUTHOR INFORMATION

Phone: +86-591-2286 6125; fax: +86-591-2286 6135

E-mail: dianping.tang@fzu.edu.cn (D. Tang)

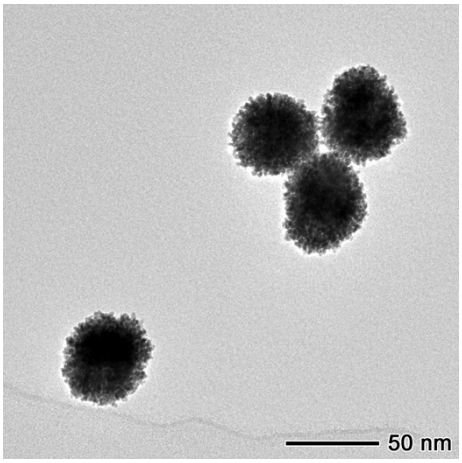

Fig. S1 TEM image of ~48.0 nm Pt nanospheres.

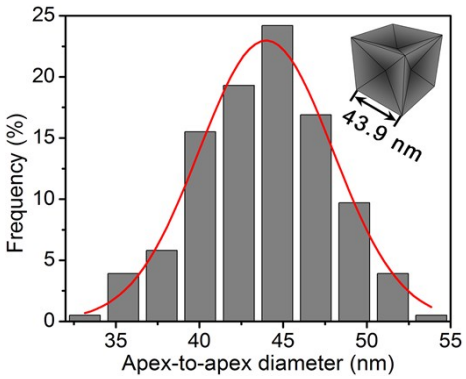

Fig. S2 Distribution of apex-to-apex diameter of the as-synthesized HIF-Pt-CNCs based on counting more than 200 particles by using "NANO MEASURER software".

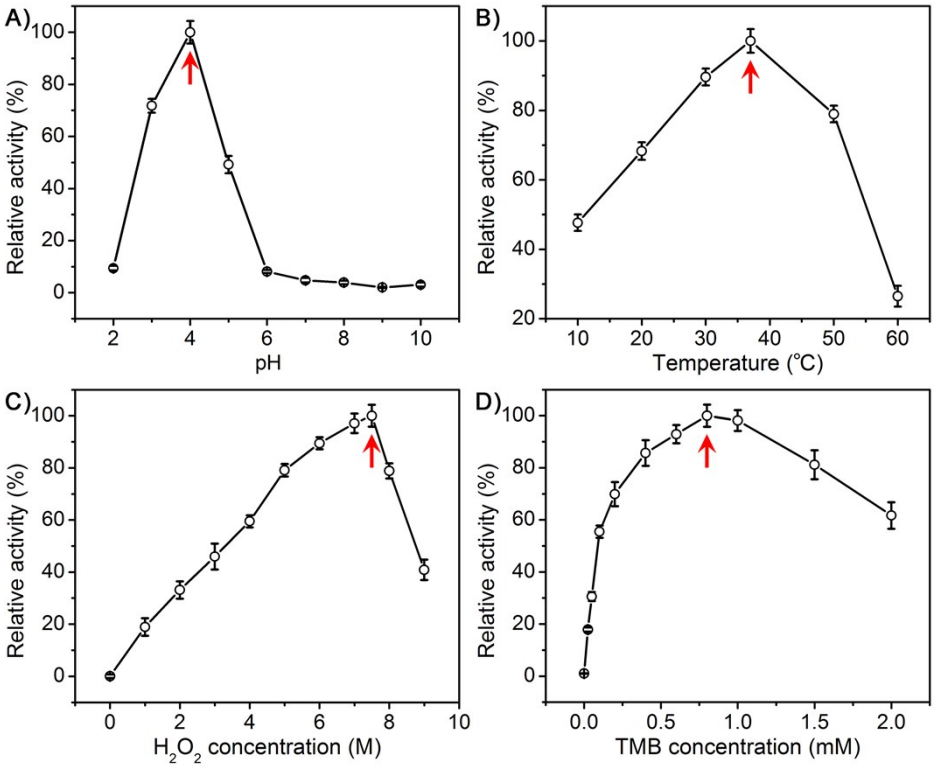

Fig. S3 The effect of pH (A), temperature (B), H_2O_2 concentration (C), and TMB concentration (D) on the peroxidase-like catalytic activity of the HIF-Pt-CNCs. The maximum point in each curve is set as 100%. Error bars indicate standard deviations (n = 3).

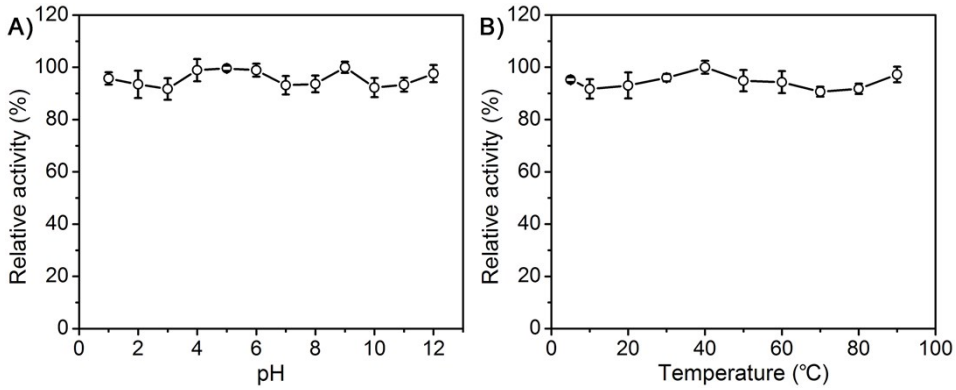

Fig. S4 Relative catalytic activities of HIF-Pt-CNCs after incubation for 2 h at various pH values (A) and temperatures (B), respectively. The maximum point in each curve is set as 100%. Error bars indicate standard deviations (n = 3).

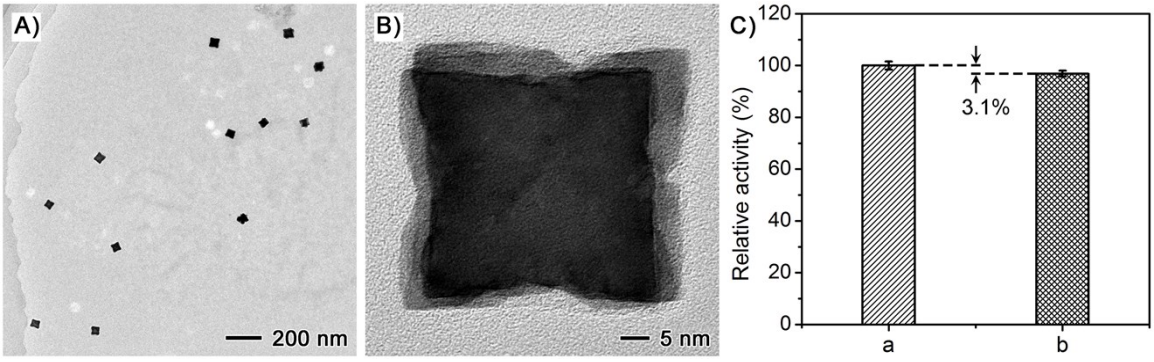

Fig. S5 (A, B) Regular TEM image (A) and HRTEM image (B) of the DAb-conjugated HIF-Pt-CNCs after the colorimetric immunoassay. (C) Relative catalytic activities of the DAb-conjugated HIF-Pt-CNCs before (a) and after (b) the colorimetric immunoassay. The activity before the colorimetric immunoassay is set as 100%. Error bars indicate standard deviations (n = 3).

The experiments were carried out as follows: i) after the colorimetric immunoassay of 300 PSA standards (20 ng mL^{-1} as an example), the detection solutions in the wells of the plates were discarded, and the wells were washed three times with water; ii) 100 μL of 0.1 M Glycine-HCl buffer (pH 2.3) was added into the wells to dissociate the antibody-antigen complexes and release the DAb-conjugated HIF-Pt-CNCs;[S1] iii) the released DAb-conjugated HIF-Pt-CNCs in the buffer were collected and washed with water twice *via* centrifugation, and the collected DAb-conjugated HIF-Pt-CNCs were dispersed in 1 mL of water; iv) the structure and morphology of these collected HIF-Pt-CNCs were characterized by TEM; and v) the catalytic activities of these collected HIF-Pt-CNCs and the unused DAb-conjugated HIF-Pt-CNCs toward H_2O_2-TMB system were determined and compared under the same conditions including the same Pt concentration (Please note that the concentrations of Pt element in the collected HIF-Pt-CNCs suspension and the unused DAb-conjugated HIF-Pt-CNCs suspension were determined to be 1.7 mg L^{-1} and 36.2 mg L^{-1}, respectively , by ICP-OES.).

Fig. S5A and B show the TEM images of the collected HIF-Pt-CNCs. It can be seen that the structure and morphology of these collected HIF-Pt-CNCs were almost the same as those of the original HIF-Pt-CNCs (Fig. 1C and D), indicating a good structural stability of HIF-Pt-CNCs during the detection process. Also the catalytic activity of the collected HIF-Pt-CNCs only decreased 3.1% compared to the activity obtained by the unused DAb-conjugated HIF-Pt-CNCs, suggesting a good catalytic stability of HIF-Pt-CNCs during the detection process (Fig. S5C).

Table S1. Projection angles and geometrical parameters of concave nanocubes bounded by different types of high-index facets.[S2]

projection direction	geometrical model of the polyhedron	equation for the projection angle	calculated projection angle	
			(*hkl*)	α
[001]	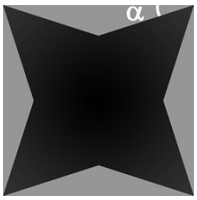	$\alpha = \arctan(k/h)$	(410)	14.0°
			(720)	15.9°
			(310)	18.4°
			(830)	20.6°
			(520)	21.8°
			(730)	23.2°

Table S2. Comparison of the kinetic parameters of various Catalysts toward the oxidation of TMB by H_2O_2.[a]

catalyst	$[E]_0$ (M)	substance	V_{max} (M s^{-1})	K_{cat} (s^{-1})	references
HRP	2.5×10^{-11}	TMB	1.0×10^{-7}	4.00×10^{3}	S3
	2.5×10^{-11}	H_2O_2	8.71×10^{-8}	3.48×10^{3}	
Fe_3O_4 nanoparticles	1.14×10^{-12}	TMB	3.44×10^{-8}	8.58×10^{4}	S3
	1.14×10^{-12}	H_2O_2	9.78×10^{-8}	3.02×10^{4}	
Co_3O_4 nanoparticles	3.43×10^{-10}	TMB	6.27×10^{-8}	1.83×10^{2}	S4
	3.43×10^{-10}	H_2O_2	1.21×10^{-7}	3.53×10^{2}	
Fe_2O_3 nanoparticles	3.09×10^{-10}	TMB	1.06×10^{-6}	3.43×10^{3}	S5
	3.09×10^{-10}	H_2O_2	1.17×10^{-6}	3.79×10^{3}	
MnO_2 nanoparticels	3.01×10^{-8}	OPD	8.21×10^{-8}	2.73	S6
	3.01×10^{-8}	H_2O_2	5.71×10^{-8}	1.90	
Au@Pt nanorods	1.25×10^{-11}	TMB	1.81×10^{-7}	1.40×10^{4}	S7
	N/A	N/A	N/A	N/A	
Au@Pd nanoparticles	9.60×10^{-11}	TMB	2.00×10^{-6}	2.10×10^{4}	S8
	9.60×10^{-11}	H_2O_2	4.40×10^{-6}	4.60×10^{4}	
Pt nanoparticles	8.12×10^{-11}	TMB	1.26×10^{-6}	2.27×10^{4}	S9
	8.12×10^{-11}	H_2O_2	1.85×10^{-6}	1.55×10^{4}	
Pd nanocubes	1.40×10^{-12}	TMB	9.70×10^{-8}	6.90×10^{4}	S10
	1.40×10^{-12}	H_2O_2	6.50×10^{-8}	4.60×10^{4}	
Pd-Ir nanocubes	3.40×10^{-14}	TMB	6.50×10^{-8}	1.90×10^{6}	S10
	3.40×10^{-14}	H_2O_2	5.10×10^{-8}	1.50×10^{6}	
HIF-Pt-CNCs	2.54×10^{-14}	TMB	1.52×10^{-7}	5.98×10^{6}	Present work
	2.54×10^{-14}	H_2O_2	1.29×10^{-7}	5.08×10^{6}	

[a] $[E]_0$ is the catalyst concentration, K_m is the Michaelis constant, V_{max} is the maximal reaction rate, and K_{cat} is the catalytic constant, where $K_{cat}=V_{max}/[E]_0$.

REFERENCE